Advanced Robotics, Vol. 21, No. 12, pp. 1441–1469 (2007)

Also available online - www.brill.nl/ar

Full paper

Intention-based walking support for paraplegia patients with Robot Suit HAL

KENTA SUZUKI [1], GOUJI MITO [1], HIROAKI KAWAMOTO [2], YASUHISA HASEGAWA [1] and YOSHIYUKI SANKAI [1,*]

[1] *Graduate School of Systems and Information Engineering, University of Tsukuba, 1-1-1 Tennodai, Tsukuba, Ibaraki 305-8573, Japan*

[2] *Japan Association for the Advancement of Medical Equipment, NKD Building, 3-42-6 Hongo, Bunkyo-ku, Tokyo 113-0033, Japan*

Received 9 January 2007; accepted 1 April 2007

Abstract—This paper proposes an algorithm to estimate human intentions related to walking in order to comfortably and safely support a paraplegia patient's walk. Robot Suit HAL (Hybrid Assistive Limb) has been developed for enhancement of a healthy person's activities and for support of a physically challenged person's daily life. The assisting method based on bioelectrical signals such as myoelectricity successfully supports a healthy person's walking. These bioelectrical signals, however, cannot be measured properly from a paraplegia patient. Therefore another interface that can estimate a patient's intentions without any manual controller is desired for robot control since a manual controller deprives a patient of his/her hand freedom. Estimation of a patient's intentions contributes to providing not only comfortable support but also safe support, because any inconformity between the robot suit motion and the patient motion results in his/her stumbling or falling. The proposed algorithm estimates a patient's intentions from a floor reaction force (FRF) reflecting a patient's weight shift during walking and standing. The effectiveness of this algorithm is investigated through experiments on a paraplegia patient who has a sensory paralysis on both legs, especially his left leg. We show that HAL supports the patient's walk properly, estimating his intentions based on the FRF, while he keeps his own balance by himself.

Keywords: Robot suit; paraplegia; walking support; intention estimation; floor reaction force.

1. INTRODUCTION

People may have muscle rigidity, relaxation, involuntary muscle contractions and sensory paralysis due to cerebral paralysis, stroke, spinal cord injury, muscular dystrophy and post-polio syndrome. Even if people do not suffer from these physical problems, aging brings various complications on their motility. Most

*To whom correspondence should be addressed. E-mail: cybernoid@golem.kz.tsukuba.ac.jp

people who have problems on the lower limbs due to these symptoms or aging are unable to walk and, at worst, are bedridden all day long. Moreover, this situation depresses a patient's feelings, e.g., bedridden patients lose their will to life. Caregivers including the patient's family also have problems looking after them once a person has motility troubles. To relieve these problems and to support the patient's independent life, it is important to provide them with a safe and convenient transportation device.

A wheelchair is now used in most cases as a transportation device for patients with gait disorder. It is convenient for the patients because they can move easily as long as enough muscular power remains in their upper body. Even if a patient has weakness of the arms, a motorized wheelchair could be used. However, wheelchairs have some problems relating to the user's environment and the user's posture. In particular, wheelchair users are apt to keep a sitting posture for a long time and have less opportunity to exercise their own lower bodies. That may cause a decrease in not only muscular power of the lower body with paralysis, but also residual physical functions. This problem could be solved if a patient with paraplegia could walk on his/her own legs as a healthy person does. Therefore, a device which helps a patient walk in their standing posture would be one of the solutions since the patient can locomote with their legs receiving physical support.

Several devices for walking support have been developed. In our study, a wearable-type robot 'Robot Suit HAL' (Hybrid Assistive Limb) has been developed in order to physically support a wearer's daily activities and heavy work. HAL-1, utilizing DC motors and ball screws as shown in Fig. 1a, was developed as the first prototype of HAL [1] and it enhanced the wearer's walking ability by amplifying the wearer's own joint torque. After developing some prototypes, HAL-3 (Fig. 1b) was developed toward a more suitable system to be used in actual daily life [2, 3]. These robot suits have a power unit on each hip and knee joint, and they support functional motions of the lower limbs with multiple joints simultaneously. After that, HAL-5 (Fig. 1c), demonstrated at the 2005 World Exposition in Aichi, was developed for whole-body support. It assists human motions involving the wearer's upper-body activities such as carrying heavy loads. Meanwhile, 'RoboKnee' [4] and 'Wearable Walking Helper' [5] have been developed to support knee motion by using linear actuators. However, it is difficult for these two devices to support a patient with paraplegia since these devices cannot support multiple joints in the lower limbs simultaneously. As an exoskeleton to assist soldiers, disaster relief workers and other emergency personnel who need to move long distances on foot, Kazerooni *et al.* [6, 7] have developed 'BLEEX' that supports a human's walking while carrying heavy loads on his/her back. This exoskeleton is not designed for welfare purposes, and it is too large and heavy (75 kg including the exoskeleton weight and maximum payload) for patients to handle as their own supporting devices in actual daily life.

To provide effective physical support according to each wearer's condition, it is necessary to strongly focus on the control algorithm as well as mechanisms of supporting devices. HAL has a cybernic control system that is a hybrid control

控制的

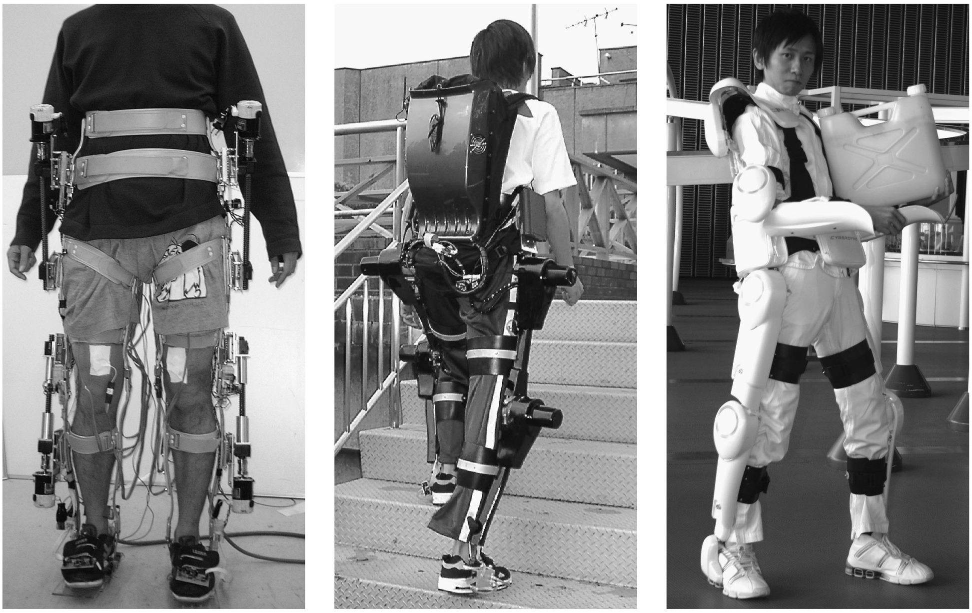

(a) HAL-1(1999). (b) HAL-3(2001). (c) HAL-5(2005).

Figure 1. Representative conventional robot suits we have developed. (a and b) HAL supports the wearer's lower-body motion. (c) HAL supports the whole-body motion. A 20-kg load is carried on a single arm.

algorithm consisting of a 'Cybernic Voluntary Control (Bio-Cybernic Control)' and 'Cybernic Autonomous Control (Cybernic Robot Control)'. The cybernic control system can provide suitable physical support to wearers in various conditions such as a healthy person, a physically challenged person, etc., by using the two algorithms as complementary controls. The features of each control algorithm are described below.

互补的

The Cybernic Voluntary Control provides physical support according to the patients's voluntary muscle activity. The power units of HAL generate power assist torque by amplifying the wearer's own joint torque estimated from his/her bioelectrical signals and the support motions are consequently controlled by signal adjustment. This control was used for power assist of a healthy person's activities [8], e.g., walking and standing up from a sitting posture, and we confirmed the Cybernic Voluntary Control successfully supported a wearer's motion. Bioelectrical signals, including myoelectricity, are useful and reliable information to estimate a human's motion intentions because the signals are measured just before corresponding visible muscle activities. Thus, the wearer receives physical support directly by an unconscious interface using the bioelectrical signals, which much more easily realize operation than manual controllers such as a joystick. HAL can physically support patients with some handicaps on their lower limbs as well as healthy people because HAL supports functional motions with multiple joints simultaneously, covering the whole of the lower limbs. However, as a whole, a patient with a gait disorder is not able to receive walking support by the Cybernic Voluntary Control because the signals that induce a broken walking pattern are not used for the power assist, and signals from the brain are not transmitted from the injured spinal cord to the more distant parts of the body and no signal is observed on the paralyzed muscles in the severest case. In that case, the Cybernic Autonomous Control can provide an effective physical support.

The Cybernic Autonomous Control autonomously provides a desired functional motion generated according to the wearer's body constitution, conditions and purposes of motion support. While bioelectrical signals are mainly used in the Cybernic Voluntary Control, various kinds of information apart from bioelectrical signals, such as reaction force and joint angle, can be used to provide comfortable physical support. It can be applied to rehabilitation and walking support for patients as well as power assist for healthy people, and it enables HAL to be used as alternate body functions for their handicaps or weakness of muscular power. In that case, HAL needs to observe a wearer's conditions and motion intentions from any motion information instead of his/her bioelectrical signals in order to provide a suitable support with a suitable moment. HAL-3 with the Cybernic Autonomous Control successfully enhances a healthy person's walking, stair-climbing, standing up from a sitting posture and cycling, synchronizing with his/her body condition [9]. In that work, floor reaction forces (FRFs) and joint angles are used as motion information to detect a wearer's conditions. Posture control, as well as sensing and recognition for an environment including a wearer are essential technologies for an entire autonomous physical support, but they remain to be solved. In this paper, the Cybernic Autonomous Control among the cybernic control systems is applied to HAL in order to support a paraplegia patient's walking. Our conventional Cybernic Autonomous Control algorithm [9] cannot be applied to them directly due to a variety of body constitutions and handicaps.

Generally, the human intentions in his/her mind are essentially independent from the physical interactions between a body and an environment. As far as we know, no current technologies can directly measure and extract the human intentions. However, we can sometimes guess human intentions in their mind from their appearance or motion. In addition, we can estimate his/her corresponding intentions if we observe a motion or an appearance that is closely connected with his/her intentions. According to conventional work on human transient walking [10, 11], a center of gravity (COG) shift to one leg is a prior motion to a walk. That motion is indispensable to swinging a leg and can be observed earlier than a bioelectrical signal such as myoelectricity, because it is observed before a human starts swinging a leg, while a bioelectrical signal is observed when the corresponding muscles start contracting. The COG shift can be used for an early and smart trigger to start walking support, because the shift is involved in preliminary motions for a walk and a human does not have to operate any manual switch to start the walking support. On the other hand, gait stopping is similar to the time-reverse motion of the gait initiation and the COG stops at around the center of both supporting legs. Therefore, this paper proposes an intention estimator that can estimate his/her walking intentions from the COG shift that is closely connected with his/her intention.

We define that intention-based support (including walking support) is to provide physical support for the wearer's next desired motion that can be predicted based on the current state or motion induced by his/her intention. In the case of walking, a human shifts the COG to a supporting leg side before he/she starts swinging a leg. If HAL can sense the COG shift induced by his/her intention, it can predict his/her walking start and then start walking support. Our project aims to realize comfortable walking support for paraplegia patients that reflect the patient's intentions on the start and stop of walking, cycle and stride of walking motion, walking direction, etc. We call the walking support conforming to these various intentions of walking 'intention-based walking support'. It is hoped that intention-based walking support improves the usability, safety and reliability of HAL. As the first step, this paper focuses on three kinds of intentions: the start and stop of walking and the beginning to swing a leg, and proposes a control algorithm that uses the patient's residual physical functions effectively. We need to observe not only the COG shift in the lateral plane, but also the forward COG shift and bending of the upper body in order to distinguish the gait initiation from other similar motions such as just stepping or changing a supporting leg for leg relaxation. However, HAL can understand the patient's intention if we instruct the wearer to shift the COG to either of his/her legs in order to receive physical support for swinging a leg. Therefore, the FRF can be one type of reliable information that reflects his/her intentions without any manual interface if a patient can control his/her weight balance in the lateral plane by holding a walking frame with their own hands.

The purpose of this study is that HAL helps a patient with paraplegia walk in a standing posture. Based on our conventional work, two additional functions should be developed for this purpose. First, HAL should generate suitable bipedal walking according to the patient's body constitution. Reference trajectories for each joint support should be designed in a different way because bioelectrical signals are not observed from a patient with paraplegia. The reference motions consist of swinging the wearer's leg, supporting his/her weight and shifting his/her weight from one leg to the other. Second, HAL should provide walking support according to the patient's intentions that are estimated from the wearer's COG shift. To achieve the two functions mentioned above, this paper takes the following approaches:

(i) To achieve bipedal locomotion partially based on walking patterns of a healthy person.

(ii) To estimate the wearer's intentions from his/her COG shift that is observed by the FRF.

(iii) To synchronize support motions with estimated wearer's intentions: walk start, stop and the beginning to swing a leg.

Section 2 explains the assumptions and approach of this study. Section 3 introduces the robot suit 'HAL-5 Type-C' used in this experiment. Section 4 describes the proposed algorithm for walking support and intention estimation. Section 5 shows experimental results and verifies the performance of the proposed algorithm in HAL-5 Type-C. Finally, Section 6 gives the conclusions.

2. ASSUMPTIONS AND APPROACH

In this paper, a proposed algorithm is applied to walking support for a paraplegia patient called 'participant A' in this paper. He has sensory and motor paralysis on both legs, especially the left leg because of spinal cord injury (SCI) caused by a traffic accident. He gave informed consent before participating and the experiments were conducted under the inspection of physical therapists. He can keep a standing posture and slowly walk by himself with two canes. In this case, we cannot measure proper bioelectrical signals to estimate his intention during walking because of the disorder of neural transmission. We, therefore, use the FRF instead of bioelectrical signals in this experiment. The FRF reflects his weight shift during walking and standing. It should be noted that he can control his balance holding a walking frame and that our algorithm can estimate his intentions from his FRF. That is, our algorithm synchronizes the physical support with his intentions through his controlled weight balance not by using manual controllers such as a joystick, but by using the FRF during walking and standing. The reference patterns for the patient are extracted from a healthy person's walk. The healthy person's walking motion could be suitable for the patient if he/she has the same body constitution as the healthy person. The extracted walking motion, however, should be adjusted according to the patient's body constitution and handicap conditions, e.g., the walking cycle and amplitude of each joint trajectory in swinging a leg.

3. ROBOT SUIT HAL

In the experiment, HAL-5 clinical type (HAL-5 Type-C) made for participant A was used. Figure 2 shows an overview of HAL-5 Type-C and Fig. 3 shows its system configurations. As in the case of the conventional type of HAL (HAL-3), HAL-5 Type-C consists of power units, exoskeletal frames, sensors and a controller. Power units are attached on each hip and knee joint, and actuate each joint by their torques. Springs are attached on the ankle joints so that the wearer's ankle joints could come back to a normal angle even if no external forces affect the joints. The spring action contributes to avoiding collisions between the toe of the swing leg and the floor. The exoskeletal frames are fixed to the wearer's legs with molded plastic bands and transmit the torques of the power units to his/her legs. There are angular sensors and FRF sensors to measure motion information of HAL-5 Type-C and a wearer to enable intention estimation for the wearer. Potentiometers as angular

归位弹簧设计

旋转电位计

(a) (b)

Figure 2. HAL-5 Type-C developed for walking support of a paraplegia patient. Total weight is 15 kg. (a) Back view. (b) Side view.

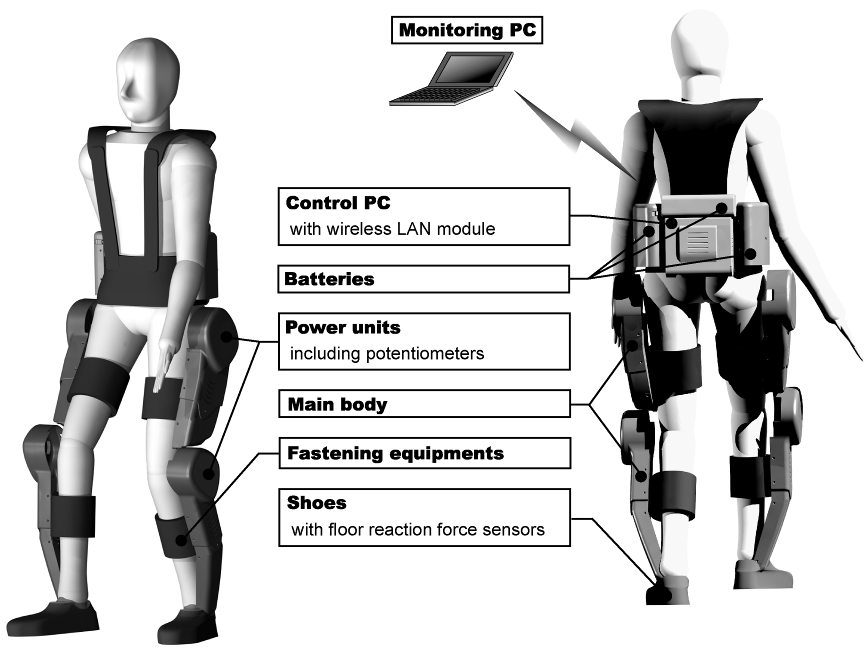

Figure 3. System configurations of HAL-5 Type-C.

sensors are attached to each joint to measure the joint angles. FRF sensors utilizing a semiconductor-type pressure sensor are implemented in shoes. Figure 4 shows the appearance of the shoes of HAL-5 Type-C with built-in FRF sensors. The weight of the wearer including HAL-5 Type-C is transferred onto the sensor unit and

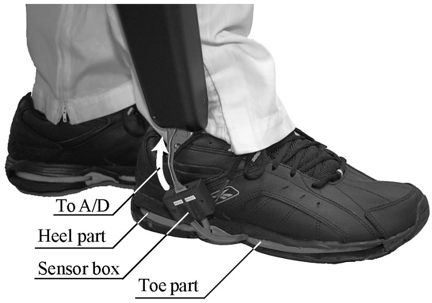

Figure 4. Built-in FRF sensors utilizing a semiconductor-type pressure sensor. These sensors can measure the distribution of load between the toe and heel parts during walking and standing because two sensors are built in the front and rear of the sole.

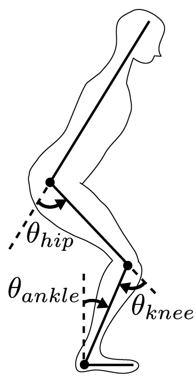

Figure 5. Rotation directions of each lower leg joint. Angle and angular velocity data shown in this paper shall be subject to a rule that flexion of a joint is a positive rotation and extension is a negative one, when the angles of each joint in an upright posture are set to the zero angles.

measured by the pressure sensors. These sensors can also measure the distribution of load between the toe and heel parts during walking and standing because two sensors are built in the front and rear of the sole. In addition, a computer and batteries are attached on a wearer's waist, and motor drivers and other electrical circuits for the signal processing are allocated on each power unit. Compared with HAL-3 (Fig. 1b), HAL-5 Type-C is improved for daily use since there is no large backpack on the user's back and the width of the power units in the back view becomes thin enough to pass through narrow spaces as shown in Fig. 2. Figure 5 shows angles and rotation directions of each joint described in this paper.

4. CONTROLLER DESIGN

In this section, we explain the controller for the walking support system. Walking motion in this work shall be considered to consist of three functions including swinging a leg, landing and supporting a body as shown in Fig. 6. In this paper, we call each span of three functions the swing phase, landing phase and support

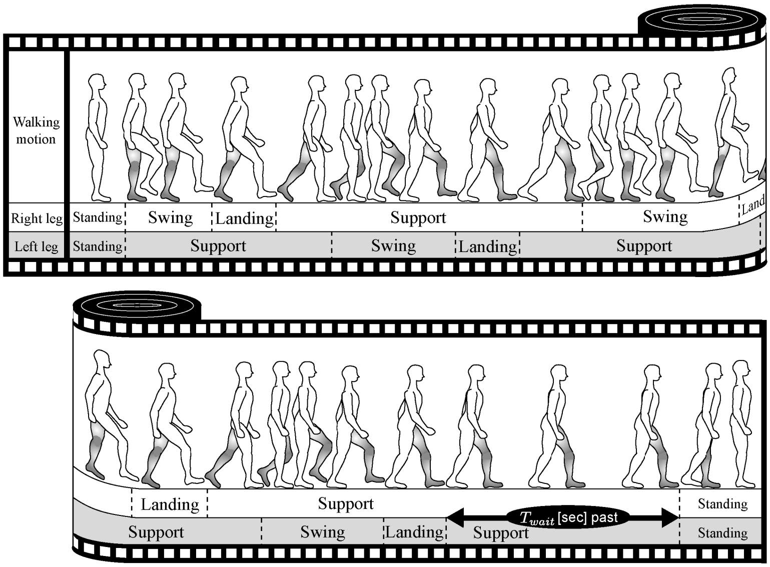

Figure 6. Three functions in walking motion: swing phase, landing phase and support phase. T_{wait} is a temporal threshold to switch the walking support to the standing posture support. If a wearer wants to stop walking in their tracks, they just have to stop weight shifting for T_{wait} seconds.

phase. In the swing phase, the patterns extracted from a healthy person's walk are applied as the reference patterns of the proportional and derivative (PD) control for the corresponding joints of a wearer. The reference patterns are used for the corresponding leg's control synchronizing with the wearer's intention estimated by our proposed algorithm. In the landing phase, we realize the leg function for a foot landing by not tracking reference patterns, but by applying constant-value control. Based on our conventional work [12], we found that the knee joint of a wearer at landing is apt to be flexed by his/her own weight and much torque beyond the torque tolerance is needed to compensate for the knee bend. Therefore, the knee joint has to be extended earlier than the reference pattern by constant-value control. In the support phase as well as the landing phase, the leg is supported by constant-value control in order to support the weight by one leg. The following sub-sections explain the details of the controller algorithm.

4.1. Reference pattern generation

As mentioned above, a swing leg in the swing phase is supported by applying reference walking patterns measured in a healthy person's walk. The reference patterns are generated in the following process:

(i) To measure angle data of the hip and knee joints in a healthy person's walk.

(ii) To divide a sequence of the measured walk pattern into patterns of each step and then average the walk patterns.

(iii) To divide the averaged pattern into three phases and extract a pattern in the swing phase.

First, we measure a healthy person's walk to acquire the angle data of hip and knee joints during walking. In this experiment, we measure the normal walk of a man in his 20s, who has a similar body constitution, including height, weight and length of legs, to participant A. Second, a sequence of the measured walk pattern is divided into patterns in each step and then the patterns averaged. At this stage, we should pay note that habits of walking and asymmetry between the right and left leg step are not strongly reflected in the extracted patterns. Figure 7a shows walking patterns in one step averaged in this experiment. Finally, the averaged walking patterns are divided into patterns in the swing, landing and support phases. The swing phase is between the moment when the foot leaves the floor and the moment when the thigh is fully flexed. The landing phase continues until the moment when the foot of the swing leg contacts the floor and the support phase continues until the moment when one step finishes. The walking patterns extracted from a healthy person's walk are shown in Fig. 7b–d. Namely, Fig. 7b shows the reference angle patterns in the swing phase used in this walking support. The PD controller to drive a leg swing needs reference angular velocity patterns as well as the angle patterns and the angular velocity patterns are generated by differentiating the angle patterns with respect to time. In addition, the time scales of the reference patterns are linearly

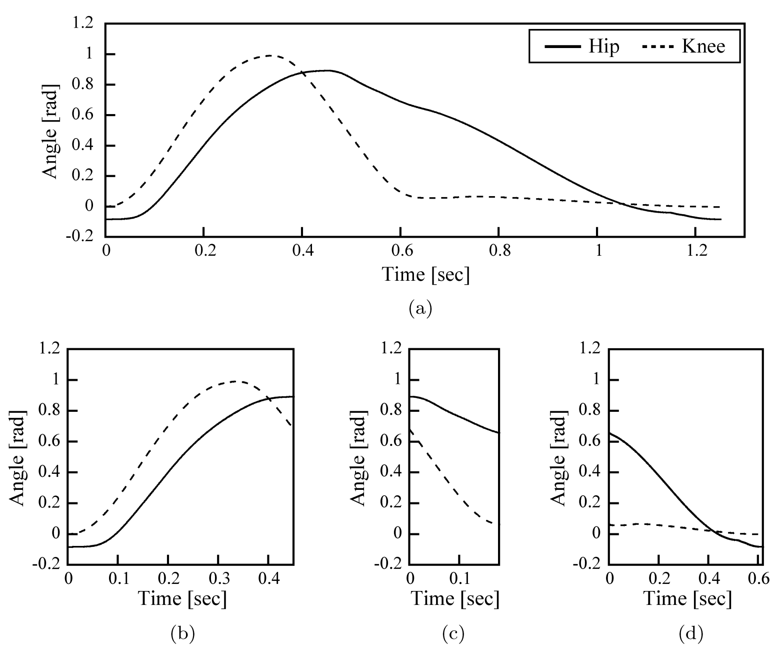

Figure 7. Reference walking patterns of joint angle. (a) Patterns in one cycle of walking. (b) Patterns in the swing phase. (c) Patterns in the landing phase. (d) Patterns in the support phase.

Table 1.
Reference values in one cycle of walking support

	Swing phase	Landing phase	Support phase
θ_{href} (rad)	Fig. 7b	0.0	0.0 (−0.7)
$\dot{\theta}_{\text{href}}$ (rad/s)	time derivative of Fig. 7b	0.0	0.0
θ_{kref} (rad)	Fig. 7b	−0.052	−0.052
$\dot{\theta}_{\text{kref}}$ (rad/s)	time derivative of Fig. 7b	0.0	0.0

shortened or lengthened so that the walking cycle could be adjusted to a wearer's intentions or a wearer's body constitution.

On the other hand, a swing leg in the landing phase is supported by constant-value control for the preparation of patient's weight support. The reference angle and angular velocity in the landing and support phases are empirically set. Table 1 shows reference values in each phase of walking support. In this table, θ_{href} and $\dot{\theta}_{\text{href}}$ show the reference angle and angular velocity of a hip joint, respectively, and θ_{kref} and $\dot{\theta}_{\text{kref}}$ show the reference angle and angular velocity of a knee joint, respectively. In addition, the hip and knee joints should be straightened through the landing and support phase in order to support the wearer's weight by one leg. Therefore, the reference angle of hip joint in the landing phase is 0 rad. Table 1, however, shows the reference angle of the knee joint is not 0 rad but −0.052 rad. This over-extension of the knee joint can prevent the knee joint from bending due to the impact of landing a foot and gravity. In general, it is quite harmful for a human to extend the knee joint excessively, but HAL does not extend wearer's joints beyond the range of motion since the fastening equipment of HAL made of rigid plastic has the little flexibility and mechanical limiters at the knee joints prevent the joints from extending more than that angle. HAL controls the joint angle to keep the reference values in the support phase until the end of the single leg support phase when the foot of the opposite side swing leg touches on a floor. After the foot of the swing leg makes contact with the floor, the reference hip joint angle of the supporting leg switches from 0.0 to −0.7 rad shown in parentheses in Table 1. This hip extension contributes to the smooth weight shift from the current supporting leg to the following one. The reference angular velocity of both joints in the landing and support phase is consistently 0.0 rad/s through one cycle of walking support.

4.2. Intention estimator

Estimation of a patient's intentions contributes to providing not only comfortable support, but also safe support, because an inconformity between the robot suit motion and the patient motion results in his stumbling or falling. Instead of bioelectrical signals used for the control of the conventional HAL, the FRF is used for intention estimation of participant A who can control his weight balance using two canes with his hands. The FRF reflects the position of the COG and the COG could be reliable information for intention estimation. For example, a leg could leave the floor and work as a swing leg safely if it does not support his/her weight.

HAL estimates which leg supports the wearer's weight when the wearer begins to swing the right or left leg and when he/she wants to stop walking. At first, for example, the right leg is considered to be the support leg when the foot contact condition:

$$f_{\mathrm{rh}} > \alpha_{\mathrm{rh}} \quad \text{or} \tag{1}$$

$$f_{\mathrm{rt}} > \alpha_{\mathrm{rt}}, \tag{2}$$

is satisfied, where f_{rh} and f_{rt} are the FRFs of the right foot heel side and toe side, respectively. In addition, α_{rh} and α_{rt} are thresholds to detect a landing of the right foot. In general, condition (1) is applied in advance of (2) since a healthy person puts the heel of the swing leg on the floor in advance of the toe. Patients with leg paralysis, such as participant A, however, have a foot weighed down and may put the toe of the swing leg on the floor in advance of the heel. Condition (2) is effective in detecting the landing in cases of paraplegia patients. On the other hand, the left leg is considered to be the support leg when the foot contact condition:

$$f_{\mathrm{lh}} > \alpha_{\mathrm{lh}} \quad \text{or} \tag{3}$$

$$f_{\mathrm{lt}} > \alpha_{\mathrm{lt}}, \tag{4}$$

is satisfied, where f_{lh} and f_{lt} are the FRFs of the left foot heel side and toe side, respectively. In addition, α_{lh} and α_{lt} are thresholds to detect landing of the left foot.

Second, for example, HAL estimates the intention that a wearer wants to swing the right leg when swing start conditions:

$$f_{\mathrm{rh}} < \beta_{\mathrm{rh}} \quad \text{and} \tag{5}$$

$$f_{\mathrm{rt}} < \beta_{\mathrm{rt}}, \tag{6}$$

are satisfied, where β_{rh} and β_{rt} are thresholds to detect the moment when each part of the right foot leaves the floor. On the other hand, HAL estimates the intention that a wearer wants to swing the left leg when swing start conditions:

$$f_{\mathrm{lh}} < \beta_{\mathrm{lh}} \quad \text{and} \tag{7}$$

$$f_{\mathrm{lt}} < \beta_{\mathrm{lt}}, \tag{8}$$

are satisfied, where β_{lh} and β_{lt} are thresholds to detect the moment when each part of the left foot leaves the floor. In this study, the following two constraint conditions are added to the above conditions for more stable estimation of the wearer's intentions:

(i) Do not start to swing a leg unless the foot of the opposite side leg is on the floor.
(ii) Do not swing the same leg sequentially.

HAL estimates the intention that a wearer wants to stop in his/her tracks if a certain time has passed before the swing start conditions (5) and (6) or (7) and (8) are satisfied. In the walking support, HAL stops the sequential walking support and helps a wearer come back to the standing posture when the condition:

$$t_{\mathrm{cur}} - t_{\mathrm{r}} > T_{\mathrm{wait}} \quad \text{or} \tag{9}$$

$$t_{\mathrm{cur}} - t_{\mathrm{l}} > T_{\mathrm{wait}}, \tag{10}$$

is satisfied, where t_{cur}, t_{r} and t_{l} are the current time and the time when the last right or left foot touched the floor. In addition, T_{wait} is a temporal threshold to switch the walking support to the standing posture support. At this moment, the reference angles of all joints are almost zero; therefore, the backward leg is replaced around the forward leg if a load on the backward leg becomes almost zero by his/her weight shift. We set $T_{\mathrm{wait}} = 5.0$ s in this experiment.

4.3. Control architecture

Bipedal locomotion using a patient's legs is achieved by tracking control and by phase synchronization of motion support with the patient's intention. This control consists of the PD control using reference walking patterns based on a healthy person's walk as shown in Fig. 7a in the swing phase and the constant-value control in the landing and support phase. Figure 8 shows a block diagram for this tracking control and phase synchronization. The human intention estimator (HIE) located in the upper-left part in Fig. 8 has the FRF as input for the estimation algorithms described in Section 4.2. Three blocks under the HIE are a library of the reference

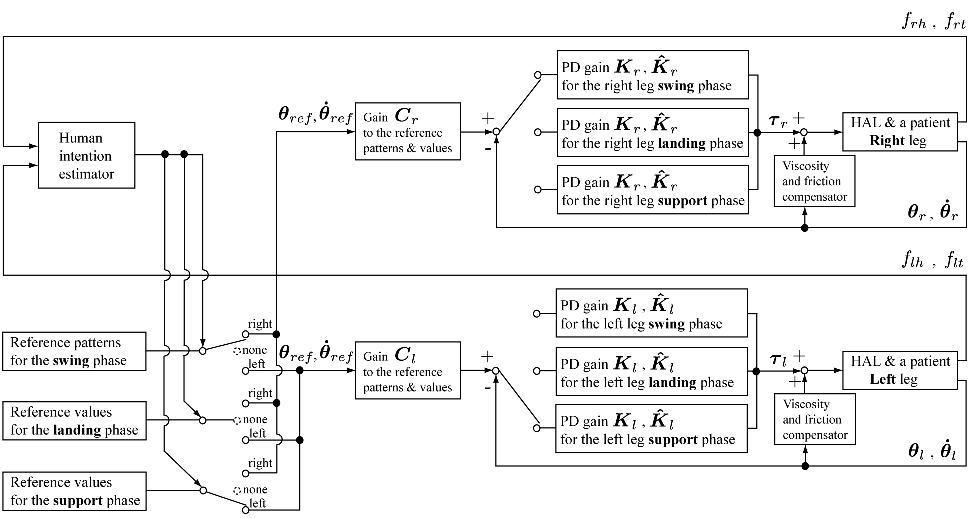

Figure 8. Block diagram for tracking control and phase synchronization. The HIE has the FRF as input for the estimation algorithms described in the previous section. Three blocks under the intention estimator are a library of the reference patterns in three walking phases, and the reference values in the landing and support phase. The intention estimator allocates these references to the two legs during walking. The ordinary PD control blocks are shown on the right side of the intention estimator and the library.

patterns in the swing phase, and the reference values in the landing and support phase. The HIE allocates these references to the two legs during walking. There are six ordinary PD control blocks on the right side of the HIE and the library. The upper three blocks are controllers for the right leg and the lower ones are for the left leg. The command voltages $\boldsymbol{\tau}_\mathrm{r}$ and $\boldsymbol{\tau}_\mathrm{l}$ to the power units on both legs are calculated by:

$$\boldsymbol{\tau}_\mathrm{r} = \mathbf{K}_\mathrm{r}(\mathbf{C}_\mathrm{r}\boldsymbol{\theta}_\mathrm{ref} - \boldsymbol{\theta}_\mathrm{r}) + \hat{\mathbf{K}}_\mathrm{r}(\mathbf{C}_\mathrm{r}\dot{\boldsymbol{\theta}}_\mathrm{ref} - \dot{\boldsymbol{\theta}}_\mathrm{r}) \tag{11}$$

and

$$\boldsymbol{\tau}_\mathrm{l} = \mathbf{K}_\mathrm{l}(\mathbf{C}_\mathrm{l}\boldsymbol{\theta}_\mathrm{ref} - \boldsymbol{\theta}_\mathrm{l}) + \hat{\mathbf{K}}_\mathrm{l}(\mathbf{C}_\mathrm{l}\dot{\boldsymbol{\theta}}_\mathrm{ref} - \dot{\boldsymbol{\theta}}_\mathrm{l}), \tag{12}$$

where $\boldsymbol{\theta}_\mathrm{r}$ and $\boldsymbol{\theta}_\mathrm{l}$ are the actual wearer's leg joint angles, $\dot{\boldsymbol{\theta}}_\mathrm{r}$ and $\dot{\boldsymbol{\theta}}_\mathrm{l}$ are angular velocities, and subscripts r and l mean right and left, respectively. In addition, $\boldsymbol{\theta}_\mathrm{ref}$ and $\dot{\boldsymbol{\theta}}_\mathrm{ref}$ are the reference joint angles and the reference angular velocities, respectively. These variables including $\boldsymbol{\tau}_\mathrm{r}$ and $\boldsymbol{\tau}_\mathrm{l}$ have two elements that correspond to two joints: the hip and knee joint. $\boldsymbol{\tau}_\mathrm{r}$, $\boldsymbol{\tau}_\mathrm{l}$, $\boldsymbol{\theta}_\mathrm{r}$, $\boldsymbol{\theta}_\mathrm{l}$, $\dot{\boldsymbol{\theta}}_\mathrm{r}$, $\dot{\boldsymbol{\theta}}_\mathrm{l}$, $\boldsymbol{\theta}_\mathrm{ref}$ and $\dot{\boldsymbol{\theta}}_\mathrm{ref}$ are given as follows:

$$\boldsymbol{\tau}_\mathrm{r} = \begin{bmatrix} \tau_\mathrm{rh} \\ \tau_\mathrm{rk} \end{bmatrix}, \quad \boldsymbol{\tau}_\mathrm{l} = \begin{bmatrix} \tau_\mathrm{lh} \\ \tau_\mathrm{lk} \end{bmatrix}, \tag{13}$$

$$\boldsymbol{\theta}_\mathrm{r} = \begin{bmatrix} \theta_\mathrm{rh} \\ \theta_\mathrm{rk} \end{bmatrix}, \quad \boldsymbol{\theta}_\mathrm{l} = \begin{bmatrix} \theta_\mathrm{lh} \\ \theta_\mathrm{lk} \end{bmatrix}, \quad \dot{\boldsymbol{\theta}}_\mathrm{r} = \begin{bmatrix} \dot{\theta}_\mathrm{rh} \\ \dot{\theta}_\mathrm{rk} \end{bmatrix}, \quad \dot{\boldsymbol{\theta}}_\mathrm{l} = \begin{bmatrix} \dot{\theta}_\mathrm{lh} \\ \dot{\theta}_\mathrm{lk} \end{bmatrix}, \tag{14}$$

$$\boldsymbol{\theta}_\mathrm{ref} = \begin{bmatrix} \theta_\mathrm{href} \\ \theta_\mathrm{kref} \end{bmatrix}, \quad \dot{\boldsymbol{\theta}}_\mathrm{ref} = \begin{bmatrix} \dot{\theta}_\mathrm{href} \\ \dot{\theta}_\mathrm{kref} \end{bmatrix}, \tag{15}$$

where subscripts rh, rk, lh and lk mean right hip joint, right knee joint, left hip joint and left knee joint, respectively. On the other hand, $\mathbf{K}_\mathrm{r}$ and $\mathbf{K}_\mathrm{l}$ are feedback gains of the joint angle errors, and $\hat{\mathbf{K}}_\mathrm{r}$ and $\hat{\mathbf{K}}_\mathrm{l}$ are feedback gains of the joint angular velocity errors. The different feedback gains are used in the swing, landing or support phase independently by adopting this control architecture. In addition, $\mathbf{C}_\mathrm{r}$ and $\mathbf{C}_\mathrm{l}$ are gains to the reference joint angles and angular velocities. These gains can adjust a joint flexion and a stride length in a wearer's supported walk. In this experiment, we set $\mathbf{C}_\mathrm{l}$ larger than $\mathbf{C}_\mathrm{r}$ in order to avoid collisions of the left leg, which has a more severe paralysis, with the floor in the swing phase. $\mathbf{K}_\mathrm{r}$, $\mathbf{K}_\mathrm{l}$, $\hat{\mathbf{K}}_\mathrm{r}$, $\hat{\mathbf{K}}_\mathrm{l}$, $\mathbf{C}_\mathrm{r}$ and $\mathbf{C}_\mathrm{l}$ are diagonal matrices which are given as follows:

$$\begin{gathered} \mathbf{K}_\mathrm{r} = \begin{bmatrix} k_\mathrm{rh} & 0 \\ 0 & k_\mathrm{rk} \end{bmatrix}, \quad \mathbf{K}_\mathrm{l} = \begin{bmatrix} k_\mathrm{lh} & 0 \\ 0 & k_\mathrm{lk} \end{bmatrix}, \\ \hat{\mathbf{K}}_\mathrm{r} = \begin{bmatrix} \hat{k}_\mathrm{rh} & 0 \\ 0 & \hat{k}_\mathrm{rk} \end{bmatrix}, \quad \hat{\mathbf{K}}_\mathrm{l} = \begin{bmatrix} \hat{k}_\mathrm{lh} & 0 \\ 0 & \hat{k}_\mathrm{lk} \end{bmatrix}, \end{gathered} \tag{16}$$

$$\mathbf{C}_\mathrm{r} = \begin{bmatrix} c_\mathrm{rh} & 0 \\ 0 & c_\mathrm{rk} \end{bmatrix}, \quad \mathbf{C}_\mathrm{l} = \begin{bmatrix} c_\mathrm{lh} & 0 \\ 0 & c_\mathrm{lk} \end{bmatrix}. \tag{17}$$

Moreover, the PD gains of swing leg control k_{rh}, k_{lh}, $\hat{k}_{\mathrm{rh}}$, $\hat{k}_{\mathrm{lh}}$, k_{rk}, k_{lk}, $\hat{k}_{\mathrm{rk}}$ and $\hat{k}_{\mathrm{lk}}$ were determined based on frequency responses and step responses of the hip and knee joints. The procedure is described in the Appendix.

The control flow for the walking support is as follows. At first, HAL supports a wearer's standing posture. Once the conditions shown in (5) and (6) are satisfied, HAL starts the PD control for the swing phase in the right leg and for the support phase in the left leg. On the other hand, HAL starts the PD control for the swing phase in the left leg and the support phase in the right leg once the conditions shown in (7) and (8) are satisfied. The PD control for a swing leg continues until HAL finishes the reference swing patterns. After that, HAL runs the constant-value control for the landing phase until the condition shown in (1) or (2) is satisfied in a case of the right leg and until the condition shown in (3) or (4) is satisfied in a case of the left leg. The other leg continues the control for the support phase. After HAL detects a contact between the foot of the swing leg and the floor, HAL runs the constant-value control for the support phase on both legs and continues the control until the next swing start conditions are satisfied. If the conditions are not satisfied, the two legs are kept at the final posture of the step. However, the reference angles of all joints are almost zero in this phase, therefore a backward leg is replaced around a forward leg if the load on the backward leg becomes almost zero by his/her weight shift. Thus, a wearer can come back to the standing posture. This algorithm can synchronize walking support with human intentions at a walk start instance, a walk stop instance as well as at the beginning of leg swing during walking. In addition to the walking support, HAL compensates for viscosity and static friction of the power units [3].

5. EXPERIMENT

The participant A is a 57-year-old male SCI patient who has incomplete sensory and motor paralysis on the left leg, especially on the left lower thigh. He is diagnosed with an incomplete SCI; the sixth and seventh thoracic vertebra (T6 and T7) are damaged. While he has good voluntary control of the upper body and limited voluntary control of both legs, he has little voluntary control of the muscles below the left knee joint. His deep sensibility, including angle sensitivity, remains partially intact in his lower thigh; however, tactile, pain and temperature sensitivities are lost. Normally, he can walk quite slowly with limping by using two canes with both his hands. During walking, however, he always feels anxious that his knee joint will suddenly and involuntarily bend during sustaining his weight as a support leg, his leg will not swing forward due to involuntary control of hip and knee flexor muscles, and he will stumble or fall down due to collisions of his 'drop foot' with the floor or the other side support leg during swinging a leg. He has trouble lifting his own leg against gravity, since he experiences significant difficulty climbing up stairs. In addition, he has stiffening of his left knee joint and sometimes spasticity of his left lower thigh muscles. He participated in our experiments more than 3 years after

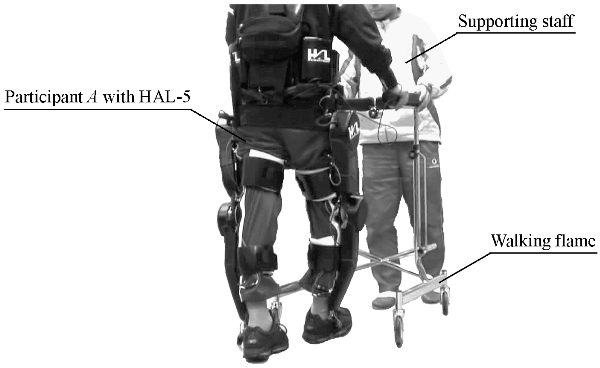

Figure 9. Experimental setting.

sustaining a SCI as a result of a traffic accident. During his admission to hospital, he received regular physical therapy for about 6 months. However, he stopped it after he left the hospital because he could not recognize any improvement in his body functions.

He gave informed consent before participating. All procedures were approved by the Institutional Review Board and the experiments were conducted under the inspection of physical therapists. The aim of HAL support is to help his leg swing forward without a limp and sustain his weight (65 kg) since he can stand with two canes by himself. This support contributes to stabilizing his walk by pushing the swing leg forward, by avoiding collisions of the swing leg with the floor and by preventing sudden knee bends. In this experiment, he walked a straight line in one direction on the flat and non-slippy floor in the laboratory. This walking support was conducted 16 times, and he was required to start walking from a standing posture and stop walking at his own convenience. In each trial, he walked 5–7 m using 12–18 steps. Moreover, he was supposed to maintain his own stability by holding a walking frame with his arms and a staff supports the walking frame for the sake of patient's safety as shown in Fig. 9, since he experienced walking support embedded with the proposed intention estimation algorithm for the first time.

5.1. Experimental setup

In this experiment, the thresholds to detect the moment when the foot leaves the floor or contacts on the floor expressed as $\alpha_{\rm rh}$, $\alpha_{\rm rt}$, $\alpha_{\rm lh}$, $\alpha_{\rm lt}$, $\beta_{\rm rh}$, $\beta_{\rm rt}$, $\beta_{\rm lh}$ and $\beta_{\rm lt}$ are finally set to 50 N based on the participant's weight and his impression after some trials. On the other hand, the feedback gains for the joint control $k_{\rm rh}$, $k_{\rm lh}$, $\hat{k}_{\rm rh}$, $\hat{k}_{\rm lh}$, $k_{\rm rk}$, $k_{\rm lk}$, $\hat{k}_{\rm rk}$ and $\hat{k}_{\rm lk}$, the gains to the reference joint angle and velocity errors $c_{\rm rh}$, $c_{\rm rk}$, $c_{\rm lh}$, and $c_{\rm lk}$ and a time span for swinging the leg are adjusted through some trials reflecting the participant's impression. The time span for swinging a leg is finally set to 0.9 s.

5.2. Results

Figures 10 and 11 show the FRF data and phase transitions on each leg during walking support. In both figures, one leg performs as the support leg up to a 'Toe off' moment when (6) or (8) is satisfied, and then the leg performs as the swing leg for 0.9 s and the leg begins to support his weight as the support leg from a 'Heel on' moment when (1) or (3) is satisfied shortly after the start of the landing phase. In addition, Fig. 12 shows the FRF data on both legs and the phase transitions at the start of walking support. The FRF of the heel part is almost zero since participant A

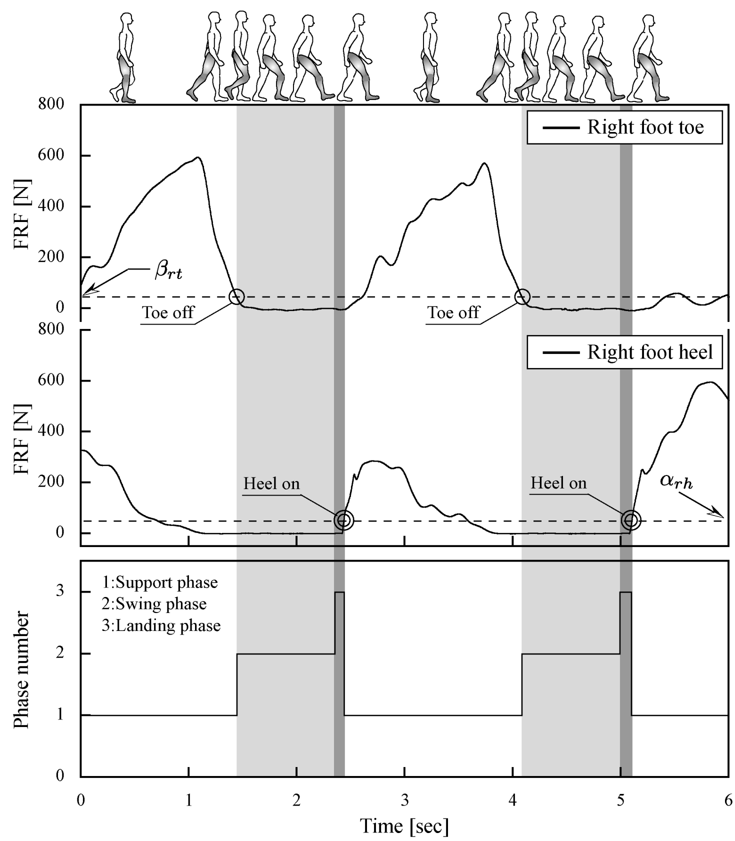

Figure 10. Result of FRF-based intention estimation on the right leg. Data in two steps of the right leg during one walking support for participant A is used. The upper two graphs show the right leg FRF data and the lower one shows right leg phase transition automatically determined through HAL's intention estimator. The right leg performs as the support leg until a 'Toe off' moment (1.4 s) when the FRF on the right toe is below the toe-off threshold β_{rt}, then the leg performs as the swing leg for 0.9 s and finally the leg begins to support his weight as the support leg from a "Heel on" moment (2.4 s) when the FRF on the right heel exceeds the heel-on threshold α_{rh} shortly after the start of the landing phase. Afterwards, the support phase was performed until the next 'Toe off' moment (4.1 s) and the support phase starts from the next 'Heel on' moment (5.1 s) again after the swing and landing phase.

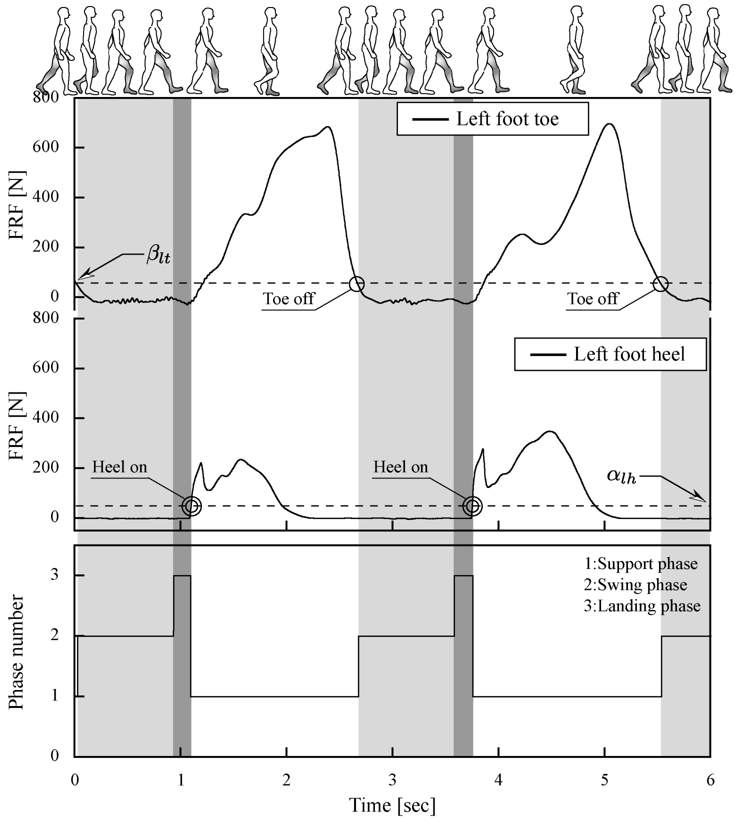

Figure 11. Result of FRF-based intention estimation on the left leg. Data in two steps of the left leg during one walking support for participant A is used. It is the data from the same walking support and in the exact same period as Fig. 10. The upper two graphs show the left leg FRF data and the lower one shows left leg phase transition automatically determined through HAL's intention estimator. The left leg supports his weight as the support leg from a 'Heel on' moment (1.1 s) when the FRF on the left heel exceeds the heel-on threshold α_{lh} until a 'Toe off' moment (2.7 s) when the FRF on the left toe is below the toe-off threshold β_{lt}, then the leg performs as the swing leg for 0.9 s and finally the leg begins to support his weight as the support leg again from the next 'Heel on' moment (3.8 s) shortly after the start of the landing phase. Afterwards, the support has been performed until the next 'Toe off' moment (5.5 s).

leans on the walking frame for the sake of safety. On the other hand, the FRF of the toe part reflects the shift of his COG. At first, he stands on his legs with a load distribution; the right leg supports about 250 N and the left leg supports about 350 N. After that, he shifts his COG in a direction toward his left side, and finally the right and left leg begin to perform as the swing leg and support leg, respectively, when (5) and (6) are satisfied. HAL starts supporting the walk of participant A synchronizing his intentions. Figures 13 and 14 show joint angles, reference and torques of the power units during walking support. Torque data was estimated based on the amount of current provided to each power unit. From the results of joint angles in these

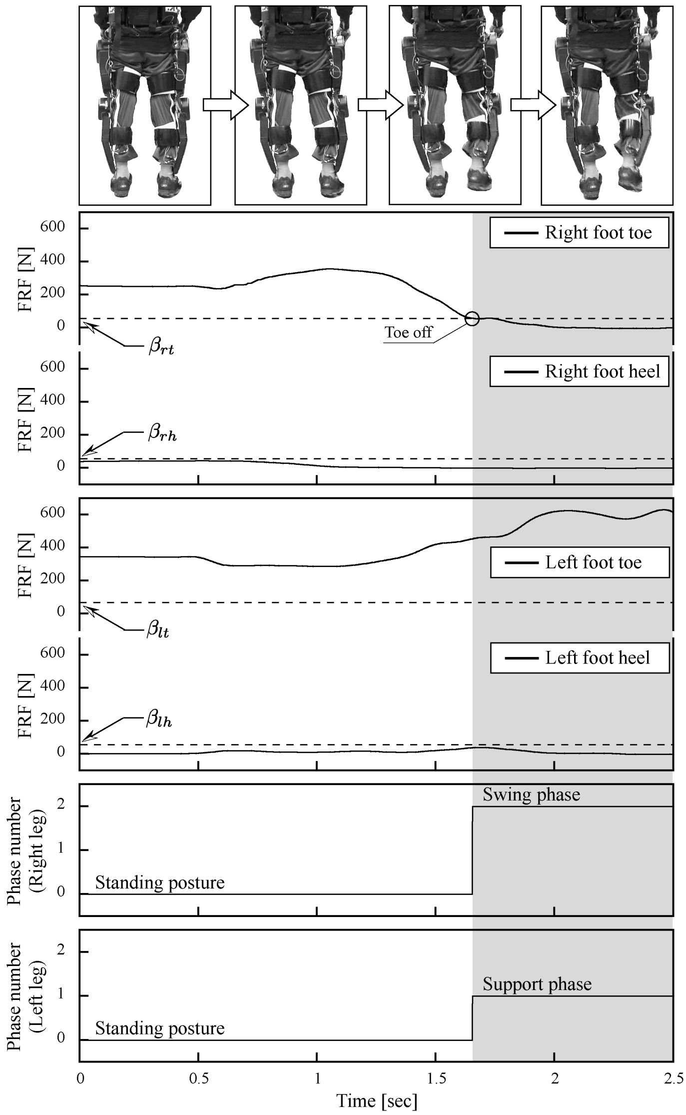

Figure 12. Start of walking support by intention estimation. The upper four pictures show the patient's weight shift onto his left leg for walk initiation. The upper two graphs below the pictures, the middle two graphs and the lower two graphs show the right leg FRF, the left leg FRF, and the right and left leg phase transitions automatically determined through HAL's intention estimator, respectively. The FRFs of both leg heel parts are almost zero since participant A leans on the walking frame, while the FRFs of both leg toe parts reflect his weight shift. At first, he stands on his legs with a load distribution; the right leg supports about 250 N and the left leg supports about 350 N. After that, he shifts his COG in a direction toward his left side, and finally the right and left leg begin to perform as the swing leg and support leg, respectively, when the FRF on the right toe is below the toe-off threshold $\beta_{\rm rt}$. HAL starts supporting his walk by synchronizing his intentions.

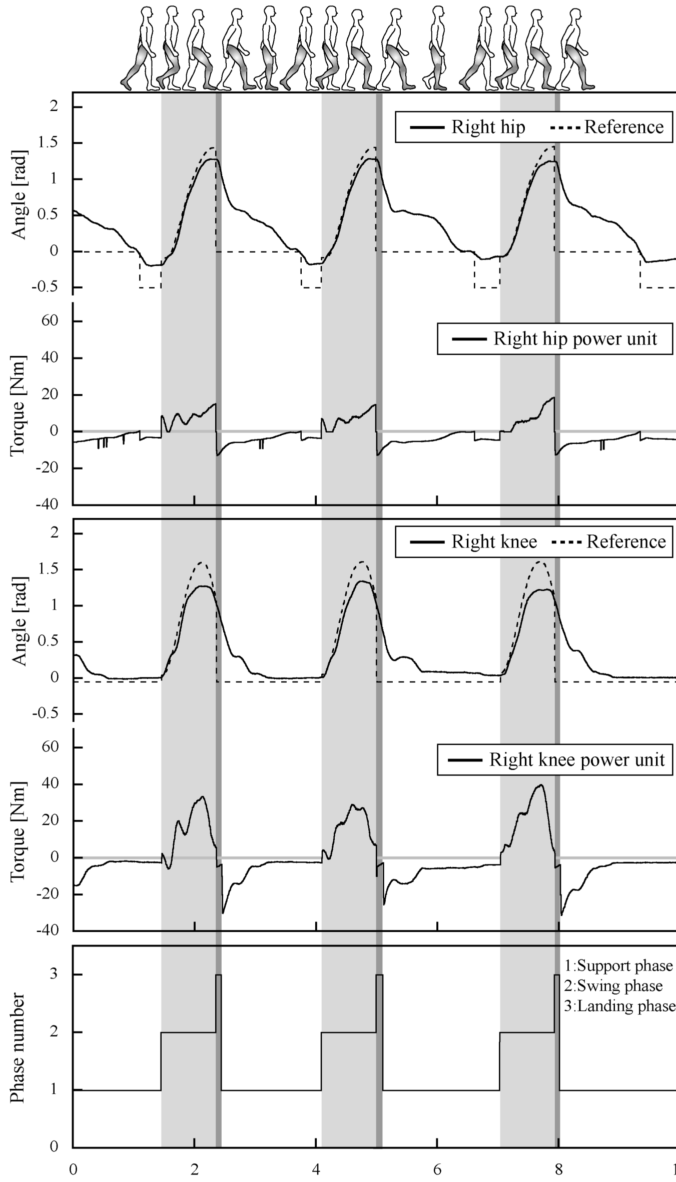

Figure 13. Right leg joint angles with reference angles and power unit torques in each phase. Data in three steps of the right leg during one walking support for participant A is used. His hip and knee joints follow the reference angles based on a healthy person's walk most of one cycle of the supported walk.

figures, his hip and knee joints follow the reference angles most of the time in one cycle of the supported walk. That means HAL supports his walk based on a healthy person's walk as shown in Fig. 7 and he performs a more natural walk with more

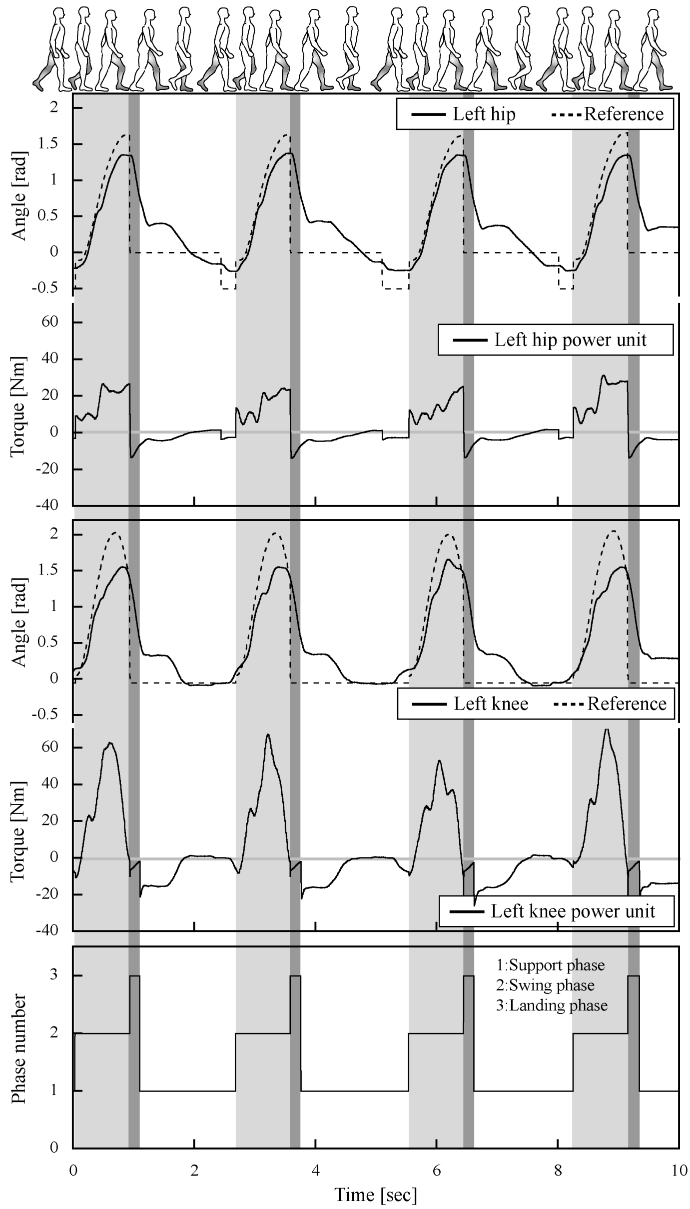

Figure 14. Left leg joint angles with reference angles and power unit torques in each phase. Data in three steps of the left leg during one walking support for participant A is used. It is the data in the same walking support and in the exact same period as Fig. 13. His hip and knee joints follow the reference angles based on a healthy person's walk most of one cycle of the supported walk. Compared to the right leg support shown in Fig. 13, his left hip and knee joints, which have more severe sensory and motor paralysis, require larger torque than his right joints.

step length than his own normal walk. HAL also successfully reduces the risk of his stumbling and falling by assisting his hip and knee flexor muscles during swinging the leg, by lifting up his drop foot, and by assisting his support leg to sustain his weight and prevent sudden knee bends. On the other hand, the results in Figs 13 and 14 show his joints do not follow the references in the latter part of the swing phases, especially the knee joint on his left leg which has more severe sensory and motor paralysis. The knee joint of participant A resists the actuator of HAL since he was used to receiving physical support. The tracking error will be small after enough training for relaxation of the knee joint in the swing phase.

6. CONCLUSIONS

In this paper, we have proposed an algorithm to estimate patients' intentions so that HAL-5 Type-C could support a patient with paraplegia to walk. The estimation algorithm based on the FRF reflecting a wearer's COG control was investigated through the walking support experiments for an incomplete SCI patient with sensory and motor paralysis on both legs. The cycle of reference walking patterns was adjusted for the patient and walking support based on the reference walking was achieved, synchronizing with a patient's intentions estimated by the algorithm. We confirmed that the algorithm successfully estimated a patient's intentions associated with the start and stop of walking, and the beginning to swing a leg based on his weight shift. HAL supported his walk based on a healthy person's walk and he performed more natural walk with more step length than his own normal walk. HAL also reduced the risk of his stumbling and falling by assisting his hip and knee flexor muscles during swinging the leg, by lifting up his drop foot and by assisting his support leg to sustain his weight and prevent sudden knee bends. The proposed walking support can be applied to whoever is able to shift his/her COG by using upper-body functions, including arms and hands, with any support equipment such as a walking frame or a cane. However, it remains to be verified whether the walking support algorithm effectively supports various types of paraplegia patients who have any problems on the lower body through experiments with other physical challenged people. It is one of our future works. In addition, in this walking support, he maintained his balance using a walking frame with his hands as he experienced the support embedded with the proposed intention estimation algorithm for the first time, while he can normally walk with two canes. He can shift his weight during the walking support with the walking frame more easily and smoothly than with his canes. The walking frame could be replaced with his own canes after he gets used to receiving HAL's physical support. In this work, HAL does not stabilize a patient's body posture. Another future work is to develop a stabilizing algorithm and mechanism so that his/her hand regains its own functions.

Acknowledgments

The authors would like to express their sincere gratitude to domestic governments including the Ministry of Education, Culture, Sports, Science and Technology of Japan and foreign governments. Thanks to their warm support, encouragement and advice, we have been making steady progress in our robot suit technology. Moreover, we thank our participants in experiments, and our project members for giving dedicated support and valuable advice with experiments.

REFERENCES

1. J. Okamura, H. Tanaka and Y. Sankai, EMG-based prototype powered assistive system for walking aid, in *Proc. Asian Symp. on Industrial Automation and Robotics*, Bangkok, pp. 229–234 (1999).
2. T. Nakai, S. Lee, H. Kawamoto and Y. Sankai, Development of powered assistive leg for walking aid using EMG and Linux, in: *Proc. Asian Symp. on Industrial Automation and Robotics*, Bangkok, pp. 295–299 (2001).
3. S. Lee and Y. Sankai, Power assist control for walking aid with HAL-3 based on EMG and impedance adjustment around knee joint, in: *Proc. IEEE/RSJ Int. Conf. on Intelligent Robots and Systems*, Lausanne, pp. 1499–1504 (2002).
4. J. E. Pratt, B. T. Krupp, C. J. Morse and S. H. Collins, The RoboKnee: an exoskeleton for enhancing strength and endurance during walking, in: *Proc. IEEE Int. Conf. on Robotics and Automation*, New Orleans, LA, pp. 2430–2435 (2004).
5. T. Nakamura, K. Saito and K. Kosuge, Control of wearable walking support system based on human-model and GRF, in: *Proc. Int. Conf. on Robotics and Automation*, Barcelona, pp. 4405–4410 (2005).
6. H. Kazerooni, R. Steger and L. Huang, Hybrid control of the Berkeley Lower Extremity Exoskeleton (BLEEX), *Int. J. Robotics Res.* **25**, 561–573 (2006).
7. R. Steger, S. H. Kim and H. Kazerooni, Control scheme and networked control architecture for the Berkeley Lower Extremity Exoskeleton (BLEEX), in: *Proc. IEEE Int. Conf. on Robotics and Automation*, Orlando, FL, pp. 3469–3476 (2006).
8. H. Kawamoto and Y. Sankai, Power assist system HAL-3 for gait disorder person, in: *Proc. Int. Conf. on Computers Helping People with Special Needs*, Linz, pp. 196–203 (2002).
9. H. Kawamoto and Y. Sankai, Power assist method based on phase sequence and muscle force condition for HAL, *Adv. Robotics* **19**, 717–734 (2005).
10. M. Sato, H. Ikeuchi, R. Katoh and T. Yamashita, Experimental analysis of reaction force and motion of center of gravity during human gait initiation (characteristics of transferring from transient phase to steady-state phase), *Trans. JSME C* **59**, 3101–3107 (1993). (in Japanese)
11. H. Ikeuchi, K. Shinkoda, R. Katoh, M. Sato and T. Yamashita, Analysis of human transient walking by wavelet transform, in: *Proc. 3rd Int. Symp. on Aritificial Life and Robotics*, Beppu, pp. 695–698 (1998).
12. K. Suzuki, Y. Kawamura, T. Hayashi, T. Sakurai, Y. Hasegawa and Y. Sankai, Intention-based walking support for paraplegia patient, in: *Proc. IEEE Int. Conf. on Systems, Man and Cybernetics*, Waikoloa, HI, pp. 2707–2713 (2005).

APPENDIX

The PD gains of swing leg control k_{rh}, k_{lh}, $\hat{k}_{\mathrm{rh}}$, $\hat{k}_{\mathrm{lh}}$, k_{rk}, k_{lk}, $\hat{k}_{\mathrm{rk}}$ and $\hat{k}_{\mathrm{lk}}$ (see (16)) were designed in preliminary experiments. In this Appendix, proportional gains for the hip joints k_{rh} and k_{lh} are expressed by $k_{*\mathrm{h}}$, and proportional gains for the knee joints k_{rk} and k_{lk} are expressed by $k_{*\mathrm{k}}$ for convenience. Derivative gains for the hip joints $\hat{k}_{\mathrm{rh}}$ and $\hat{k}_{\mathrm{lh}}$ are expressed by $\hat{k}_{*\mathrm{h}}$, and derivative gains for the knee joints $\hat{k}_{\mathrm{rk}}$ and $\hat{k}_{\mathrm{lk}}$ are expressed by $\hat{k}_{*\mathrm{k}}$.

Figure A1 shows experimental environments, where one leg can swing freely and the other leg supports the participant's weight. At first, the hip or knee joint is controlled by the PD feedback control to examine the frequency response. The reference joint angle patterns are expressed by a sine function with seven different frequencies, ranging from 0.1 to 3.0 Hz, and with 1.0 rad peak-to-peak amplitude. Five different PD gains, with the proportional gain from 20.0 to 200.0 and the derivative gain from 0.02 to 0.20, were tested. Figures A2 and A3 show the frequency responses of hip and knee joints on Bode plots. Then, a unit step response of each joint is examined with six different PD gains. Figures A4 and A5 show the responses of hip and knee joints. From the viewpoint of amplitude characteristics, resonance frequency and phase shift on the hip joint shown in Fig. A2, sufficient response could be obtained when the range that $k_{*\mathrm{h}}$ was 100.0–200.0 and $\hat{k}_{*\mathrm{h}}$ was 0.10–0.20 at less than 0.5 Hz, which equaled the leg swing frequency in this walking support. In addition, Fig. A4 shows little overshoot and sufficient convergence at the proportional gain of $k_{*\mathrm{h}} = 100.0$ and the derivative gain of $\hat{k}_{*\mathrm{h}} = 0.10$ for the unit step response. In consideration of those results, we set the hip joint feedback

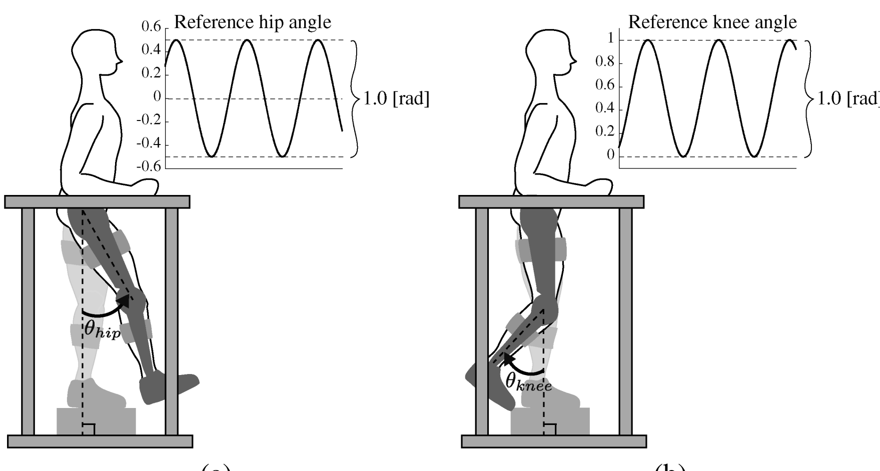

Figure A1. Experimental settings for each joint frequency response. A participant with HAL stands inside a frame with one leg on a raised block so that the other leg can swing freely. The participant is asked to keep the upper body upright and completely relax the leg to follow reference joint motions produced by the power units. Two sine curves show the reference joint angle patterns on each joint. (a) Experimental motion for hip joint. (b) Experimental motion for knee joint.

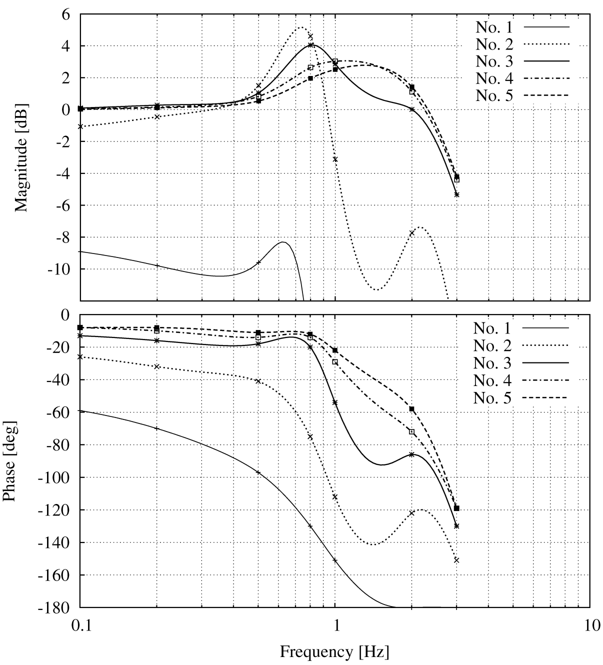

Figure A2. Frequency response of the hip joint shown in a Bode plot. The upper and lower graphs show amplitude and phase characteristics, respectively. Line 1 is a characteristic curve in the case of $k_{*\mathrm{h}} = 20.0$ and $\hat{k}_{*\mathrm{h}} = 0.02$. Similarly, lines 2–5 are for $k_{*\mathrm{h}} = 50.0$ and $\hat{k}_{*\mathrm{h}} = 0.05$, $k_{*\mathrm{h}} = 100.0$ and $\hat{k}_{*\mathrm{h}} = 0.10$, $k_{*\mathrm{h}} = 150.0$ and $\hat{k}_{*\mathrm{h}} = 0.15$, and $k_{*\mathrm{h}} = 200.0$ and $\hat{k}_{*\mathrm{h}} = 0.20$, respectively. All five lines are drawn using a cubic spline curve in order to express the correspondence with seven points in the same set of feedback gains. They, therefore, interpolate the experimental data and would not precisely express the real values.

gains $k_{*\mathrm{h}}$ and $\hat{k}_{*\mathrm{h}}$ to 100.0 and 0.10 in the actual walking support. In the same way, sufficient response was observed when $k_{*\mathrm{k}}$ was 100.0–200.0 and $\hat{k}_{*\mathrm{k}}$ was 0.10–0.20 at less than 1.0 Hz on the knee joint, as shown in Fig. A3. We also set the knee joint feedback gains as 100.0 and 0.10 from the viewpoint of overshoot and oscillation on the step response, as shown in Fig. A5.

ABOUT THE AUTHORS

Kenta Suzuki received the ME degree from the University of Tsukuba, Japan, in 2005. He is currently engaged in the development of HAL and research on Activities of Daily Living support for physically challenged people, and is working toward his PhD at the Graduate School of Systems and Information Engineering, University of Tsukuba. His research interests include biomedical engineering, rehabilitation engineering and 'cybernics'. He received the SICE Young Authors Award from the Society of Instrument and Control Engineers in 2007. He is a member of the IEEE, Robotics Society of Japan, and Society of Instrument and Control Engineers.

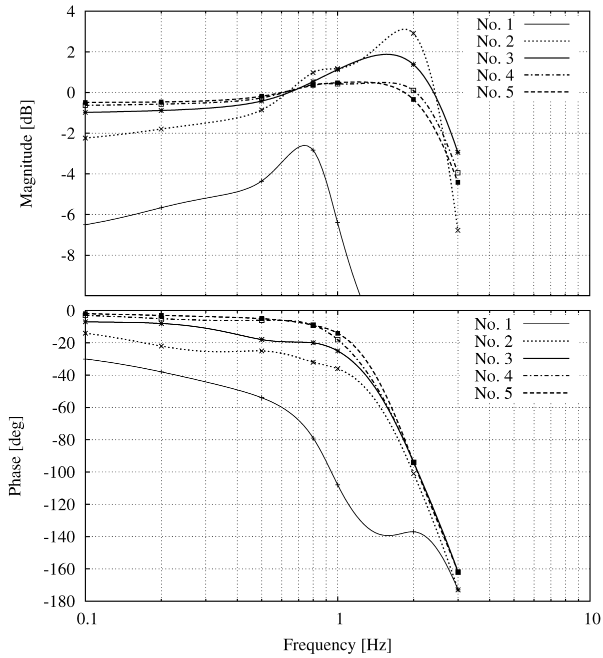

Figure A3. Frequency response of the knee joint shown in a Bode plot. The upper and lower graphs show amplitude and phase characteristics, respectively. Line 1 is a characteristic curve in the case of $k_{*\mathrm{k}} = 20.0$ and $\hat{k}_{*\mathrm{k}} = 0.02$. Similarly, lines 2–5 are for $k_{*\mathrm{k}} = 50.0$ and $\hat{k}_{*\mathrm{k}} = 0.05$, $k_{*\mathrm{k}} = 100.0$ and $\hat{k}_{*\mathrm{k}} = 0.10$, $k_{*\mathrm{k}} = 150.0$ and $\hat{k}_{*\mathrm{k}} = 0.15$, and $k_{*\mathrm{k}} = 200.0$ and $\hat{k}_{*\mathrm{k}} = 0.20$, respectively. All five lines are drawn using a cubic spline curve in order to express the correspondence with seven points in the same set of feedback gains. They, therefore, interpolate the experimental data and would not precisely express the real values.

Gouji Mito received the BE and ME degrees from the University of Tsukuba, Japan, in 2004 and 2006, respectively. From 2003 to 2006, he engaged in the project of HAL and contributed to the development of Cybernic Autonomous Control for HAL. He currently works at SECOM Co., Ltd, Japan.

Hiroaki Kawamoto received the ME and PhD degrees from the University of Tsukuba, Japan, in 2000 and 2004, respectively. He was a Research Assistant at the University of Tsukuba Venture Business Laboratory in 2004. Currently, he is a Research Resident at Japan Association for the Advancement of Medical Equipment, mainly engaged in the development of robot suits, and research on enhancement and support of human body functions. His research interests include biomechanics, biorobotics and the human–machine interface, especially human support robots. He received the Best Paper Award from the Robotics Society of Japan in 2006. He is a member of the Robotics Society of Japan and Japan Society of Mechanical Engineers.

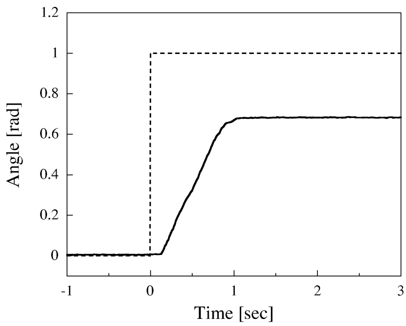

(a) $k_{*h} = 20.0, \hat{k}_{*h} = 0.02.$

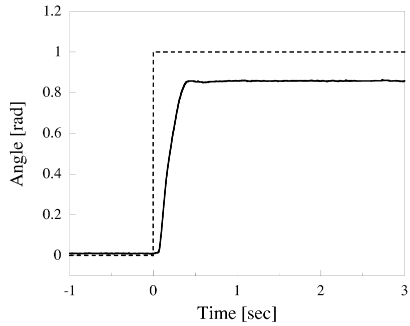

(b) $k_{*h} = 50.0, \hat{k}_{*h} = 0.05.$

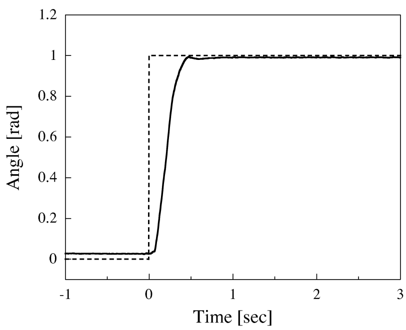

(c) $k_{*h} = 100.0, \hat{k}_{*h} = 0.10.$

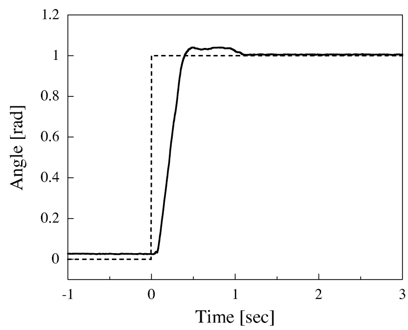

(d) $k_{*h} = 150.0, \hat{k}_{*h} = 0.15.$

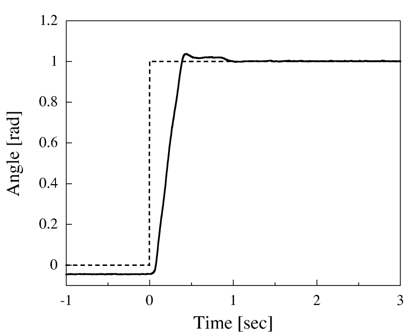

(e) $k_{*h} = 200.0, \hat{k}_{*h} = 0.20.$

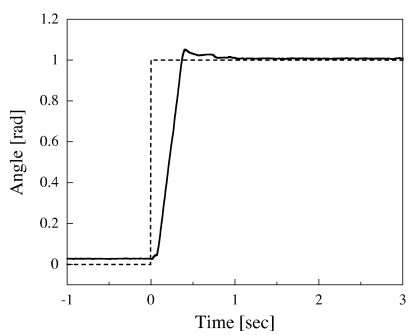

(f) $k_{*h} = 300.0, \hat{k}_{*h} = 0.30.$

Figure A4. Step responses of the hip joint on six kinds of feedback gains (PD gains). Dashed lines and solid lines in the graphs show step inputs and actual angular variations, respectively.

Yasuhisa Hasegawa received the BE and ME degrees from Nagoya University, Japan, in 1994 and 1996, respectively. From 1996 to 1998, he worked for Mitsubishi Heavy Industries Ltd, Japan. He joined Nagoya University in 1998 and received the Doctor degree from Nagoya University in 2001. He moved to Gifu University in 2003. He is currently an Assistant Professor at the University of Tsukuba, mainly engaged in the research fields of motion assistive systems, dynamic motion control and dexterous robotic hands. He is a member of the IEEE, Japan Society of Mechanical Engineers, Robotics Society of Japan, Society of Instrument and Control Engineers, and Japan Society for Fuzzy Theory and Intelligent Informatics.

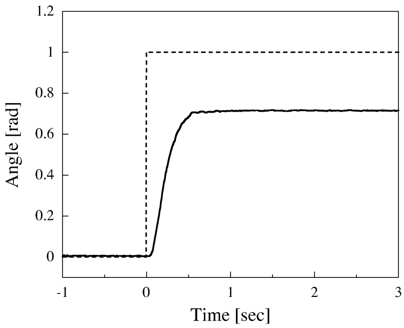

(a) $k_{*k} = 20.0, \hat{k}_{*k} = 0.02.$

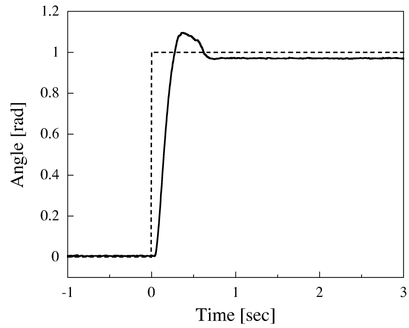

(b) $k_{*k} = 50.0, \hat{k}_{*k} = 0.05.$

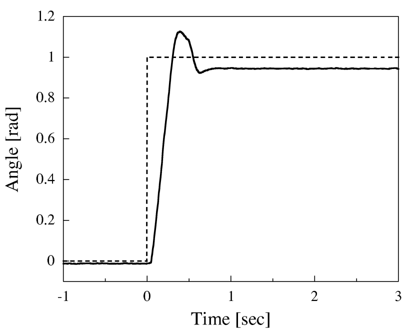

(c) $k_{*k} = 100.0, \hat{k}_{*k} = 0.10.$

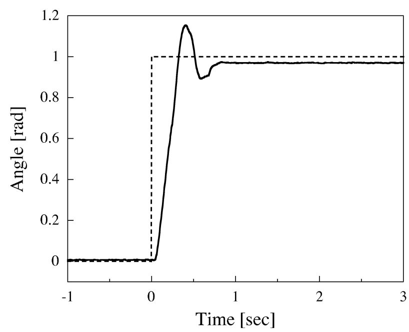

(d) $k_{*k} = 150.0, \hat{k}_{*k} = 0.15.$

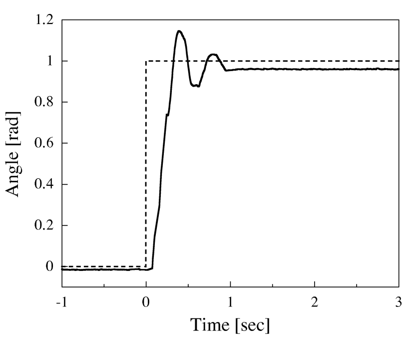

(e) $k_{*k} = 200.0, \hat{k}_{*k} = 0.20.$

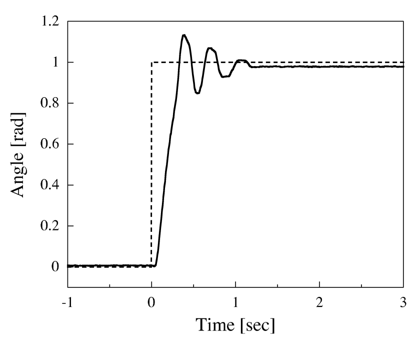

(f) $k_{*k} = 300.0, \hat{k}_{*k} = 0.30.$

Figure A5. Step responses of the knee joints on six kinds of feedback gains (PD gains). Dashed lines and solid lines in the graphs show step inputs and actual angular variations, respectively.

Yoshiyuki Sankai received the PhD in Engineering from the University of Tsukuba, Japan, in 1987. He was a Japan Society for the Promotion of Science Research Fellow, Assistant Professor, Associate Professor and Professor of Institute of Systems and Engineering in the University of Tsukuba, and a Visiting Professor at Baylor College of Medicine in USA. Currently, he is a Professor of the Graduate School of Systems and Information Engineering in the University of Tsukuba, a Director of UTARC (University of Tsukuba, Division of Advanced Robotics and Cybernics), and a President of CYBERDYNE Inc. He was/is also a President of the Japan Society of Embolus Detection and Treatment, a Chairman of the International Journal of the Robotics Society of Japan (RSJ), a Member of the Awards Committee of the RSJ, an executive Board Member of the RSJ, and an Executive Editor of *Vascular Lab. Journal.* Now he has become the creator of the world's most advanced robotic technology, HAL, which was introduced by him to the former Prime Minister and his Cabinet members in the Council for Science and Technology Policy at the Prime Minister's office, in 2006. His research interests include the new robotics frontier, 'cybernics': the next generation artificial heart, humanoid control, biomedical science, network medicine, etc. He won the World Technology Award in 2005, Good Design Gold Award in 2006, the 2006 Japan Innovator Award, the Best Paper Award from the Robotics Society of Japan in 2006, Awards from the American Society for Artificial Organs, Award from the International Society for Artificial Organs, etc. Recently, he obtained large Grants from NEDO (Ministry of Economy, Trade and Industry of Japan), large Grants for health science (Ministry of Health, Labor and Welfare of Japan) and a large grant-in-aid scientific research (Ministry of Education, Culture, Sports, Science and Technology of Japan). Now, he is promoting to apply HAL to senior citizens or physically challenged people.